

Novel Thermochromism Relating to Supramolecular Cuprophilic Interaction: Design, Synthesis, and Luminescence of Copper(I) Pyrazolate Trimer and Polymer

Jing-Xiang Zhang,[†] Jun He,[‡] Ye-Gao Yin,^{*†} Mei-Hong Hu,[†] Dan Li,[†] and Xiao-Chun Huang[†]

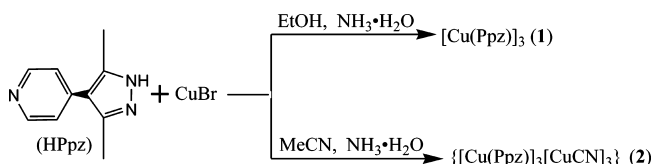
Department of Chemistry, Shantou University, Guangdong 515063, People's Republic of China, and Department of Biology and Chemistry, City University of Hong Kong, 83 Tat Chee Avenue, Kowloon, Hong Kong, People's Republic of China

Received November 6, 2007

Solvothermal reactions of 4-(pyrid-4'-yl)-3,5-dimethylpyrazole (HPpz) with CuBr in two mixed solvents, NH₃·H₂O/EtOH and NH₃·H₂O/MeCN, afforded respectively a copper(I) trimer, [Cu(Ppz)]₃ (**1**), and a polymer, {[Cu(Ppz)]₃[CuCN]₃} (**2**), both containing the [Cu(Ppz)]₃ entity as a building block. The products were found to be photoluminescent and, more interestingly, when cooled from room temperature to 10 K, they showed a blue shift followed by a red shift (hereafter shortened to a red-after-blue shift) of emission.

Recently, the triangular M₃L₃ (M = Cu, Ag, Au) complexes have received extensive attention because of their rich stacking modes in the crystal lattice and their fascinating optical properties.^{1,2} Especially, those containing the trinuclear copper(I) pyrazolate as the coordination center, for their cheap cost and peculiar photoresponse, have received the most attention.² The systems are structurally identified, including a stable nine-membered Cu₃N₆ ring and, in crystal packing, showing supra- and intermolecular cuprophilic interactions. It has been proven that the tricopper center of complexes is responsible for the solid luminescence. For example, Dias et al.,² on the basis of a photophysical study on [Cu(3-R, 5-R'-pz)]₃ (**Cu₃**; R, R' = CH₃, CF₃, Ph, i-Pr; pz

Scheme 1. Synthetic Strategy of **1** and **2**



= pyrazole), discovered an intriguing luminescence chromism of these species with variation of the temperature, solvent, and solution concentration. Mechanistically, they attributed this to a complex effect of reaction conditions on the cuprophilic interactions.

However, so far, the bulk of the studies have mainly focused on the 0D oligomers, leaving the 3D coordination polymer based on the M₃ unit much less developed.³ In a rare effort, we reported previously a Cu₃-based luminescent metal–organic framework (MOF),^{3a} therein illustrating a synthetic strategy by introducing a Cu₃ motif as a functional carrier to construct the photoluminescent MOF. To carry forward this strategy, the work used a pyridine-functionalized pyrazole, 4-(pyrid-4'-yl)-3,5-dimethylpyrazole (HPpz),⁴ as the ligand to react with CuBr in two different solvent conditions (Scheme 1). Consequently, a Cu₃-centered trimer [Cu(Ppz)]₃ (**1**) and a trimer-based polymer {[Cu(Ppz)]₃[CuCN]₃} (**2**) were obtained. The complexes, as expected, are luminescent. However, surprisingly, when the samples were cooled from room temperature to 10 K, they showed a red-after-blue shift of emission, which had never been documented before. Herein, we demonstrate the novelty of **1** and **2** by describing their syntheses, crystal structures, and variable-temperature solid luminescence.

1 was obtained as yellow air-stable crystals from heating of a EtOH/NH₃·H₂O solution of HPpz and CuBr (see the

* To whom correspondence should be addressed. E-mail: yg Yin@stu.edu.cn.

[†] Shantou University.

[‡] City University of Hong Kong.

- (1) (a) For examples, see: Balch, A. L.; Olmstead, M. M.; Vickery, J. C. *Inorg. Chem.* **1999**, *38*, 3494–3499. (b) Olmstead, M. M.; Jiang, F.; Attar, S.; Balch, A. L. *J. Am. Chem. Soc.* **2001**, *123*, 3260–3267. (c) Hayashi, A.; Olmstead, M. M.; Attar, S.; Balch, A. L. *J. Am. Chem. Soc.* **2002**, *124*, 5791–5795. (d) Singh, K.; Long, J. R.; Stavropoulos, P. *J. Am. Chem. Soc.* **1997**, *119*, 2942–2943. (e) Vickery, J. C.; Olmstead, M. M.; Fung, E. Y.; Balch, A. L. *Angew. Chem., Int. Ed. Engl.* **1997**, *36*, 1179. (f) Wang, X.-L.; Qin, C.; Wang, E.-B.; Su, Z.-M.; Li, Y.-G.; Xu, L. *Angew. Chem., Int. Ed.* **2006**, *45*, 7411–7414.
- (2) (a) For examples, see: Dias, H. V. R.; Diyabalanage, H. V. K.; Eldabaja, M. G.; Elbjairami, O.; Rawashdeh-Omary, M. A.; Omary, M. A. *J. Am. Chem. Soc.* **2005**, *127*, 7489–7501. (b) Omary, M. A.; Rawashdeh-Omary, M. A.; Alexander Gonser, M. W.; Elbjairami, O.; Grimes, T.; Cundari, T. R. *Inorg. Chem.* **2005**, *44*, 8200–8210.

- (3) (a) Only three coordination polymers based on M₃ units are documented in the Cambridge Structure Database. He, J.; Yin, Y.-G.; Wu, T.; Li, D.; Huang, X.-C. *Chem. Commun.* **2006**, *27*, 2845–2847. (b) Zhang, J.-P.; Horike, S.; Kitagawa, S. *Angew. Chem., Int. Ed.* **2007**, *46*, 889–892. (c) Enomoto, M.; Kishimura, A.; Aida, T. *J. Am. Chem. Soc.* **2001**, *123*, 5608–5609.

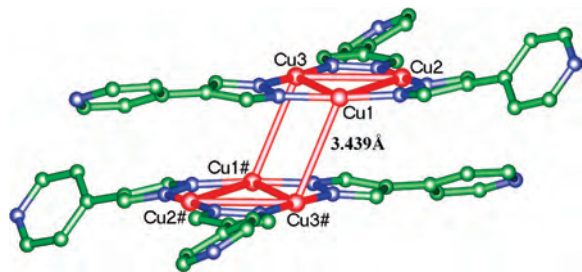


Figure 1. Perspective drawing of a dimeric $\{[Cu(Ppz)]_3\}_2$, showing its stagger assembly and the intra- and inter- Cu_3 cuprophilic interactions (red stick). Color code: Cu, red; N, blue; C, green. The methyl groups on the pyrazole rings and all of H atoms are omitted for clarity. Symmetry code: $-x, -y, 2 - z$.

Supporting Information). X-ray diffraction⁵ revealed a 0D trimer, featuring a Cu_3 core embraced by three peripheral pyridyls (Figure S1 in the Supporting Information) that are potentially capable of binding more metal ions. The central Cu_3N_6 ring of **1** is nearly coplanar with a mean deviation of 0.0393 \AA , in which the Cu^I ions are separated by $3.172\text{--}3.230 \text{ \AA}$, very close to those of the known Cu_3 -based complexes.² In the crystal lattice, the molecules of **1** are stacked in pairs (Figure 1), giving a short inter- Cu_3 $Cu \cdots Cu$ distance (3.439 \AA), smaller than those of $Cu[3\text{-(CF}_3\text{)}_5\text{-(Me)ppz}]_3$ and $Cu[3,5\text{-(CF}_3\text{)}_2\text{ppz}]_3$,² and so suggesting an intermolecular cuprophilic interaction. On the other hand, the $Cu \cdots Cu$ distance of **1**, compared with those of $\{Cu[3,5\text{-(Me)}_2\text{ppz}]_3$ and $Cu[3\text{-(CF}_3\text{)}_5\text{ppz}]_3$,² is remarkably longer, suggesting a repulsion among the pyridyls on the paired trimers. In view of crystal engineering, these facts imply that tuning the intertrimer $Cu \cdots Cu$ separation and further the emission property of a MOF by changing the substituent on the pyrazole ring is possible.

2 resulted from a reaction of HPPz with CuBr in MeCN/ $NH_3 \cdot H_2O$. Using acetonitrile as a solvent led to the involvement of CN^- , in situ generated from the C–C bond split of MeCN,⁶ as a building block in the construction of **2**. Interestingly, the CN-enabled architecture also contained $[Cu(Ppz)]_3$ units, each as a tritopic metalloligand, binding three Cu^I atoms (Cu3, Cu3A, and Cu4; Figure S1 in the Supporting Information). The trimer, like **1**, also includes a quasi-planar Cu_3N_6 ring with a mean deviation of 0.0555 \AA and shows the intra- Cu_3 cuprophilic interactions guaranteed by the $Cu \cdots Cu$ distances (3.249 and 3.128 \AA). The resemblance of the $[Cu(Ppz)]_3$ unit in **2** to that in **1** suggests

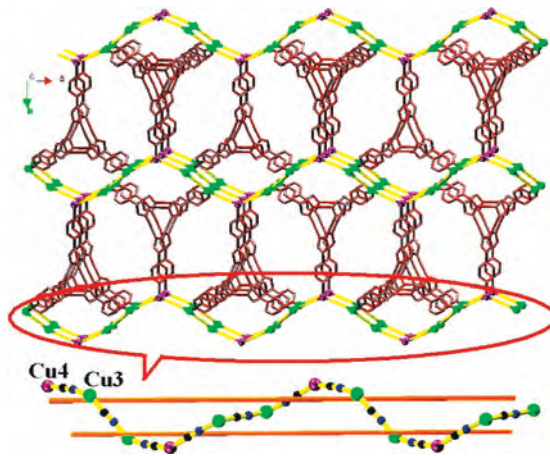


Figure 2. Presentation of a single porous network of **2** constructed from $[Cu(Ppz)]_3$ units and $[CuCN]_n$ chains. Methyl and H atoms are omitted for clarity. Color code: brown, $[Cu(Ppz)]_3$ unit; black: C; blue: N.

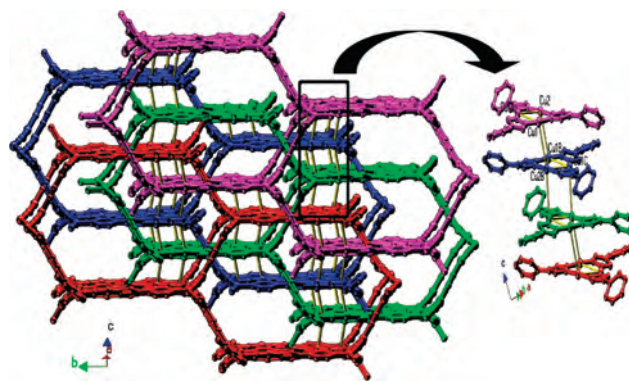


Figure 3. 4-fold interpenetration network of **2** with the $[Cu_3]_n$ chains formed by internet cuprophilic interactions ($Cu \cdots Cu = 3.317 \text{ \AA}$).

a stability of the $Cu\text{--}pz$ configuration, which promises the feasibility of predesigning the Cu_3 motif and introducing it as a functional carrier into a MOF.

Under the direction of $[Cu(Ppz)]_3$ units, the $Cu\text{--}CN$ combination in **2** gives the twist-drill polymeric chains (Figure 2), in which the cyanides act as bitopic linkers, each connecting two Cu^I atoms, and Cu3 and Cu4 are coordinated by a N_{py} and two X_{CN} ($X = C/N$) atoms. Incorporation of the $[Cu(Ppz)]_3$ units and the $[CuCN]_n$ chains generates a porous 3D framework, presenting hexameric loops, sized as $12 \text{ \AA} \times 18 \text{ \AA}$, and decameric loops, sized as $10 \text{ \AA} \times 28 \text{ \AA}$ (Figure S2 in the Supporting Information). When the Cu3 and Cu4 atoms and $[Cu(Ppz)]_3$ entities are denoted as three-connected nodes and the $CN\text{--}Cu$ and $N_{py}\text{--}Cu$ bonds as linkers, the framework of **2** is reduced to a binodal $(6^2 \cdot 10)_2(6 \cdot 10^2)$ topologized network, similar to the one we reported previously.^{3a,7} The large voids in the framework of **2** results in a 4-fold interpenetration, illustrated in Figure 3. In the $[2 + 2]$ entanglement⁸ of networks, the two equivalents in a set are related by a translation vector, $[1, 0,$

(4) Cui, Q.; Cao, X.-Y.; Tang, L.-F. *Polyhedron* **2005**, *24*, 209.

(5) Crystal data for **1**: $C_{30}H_{30}Cu_3N_9$, $M_r = 707.28$, triclinic, space group $P\bar{1}$ (No. 2), $a = 10.483(6) \text{ \AA}$, $b = 11.730(6) \text{ \AA}$, $c = 11.891(6) \text{ \AA}$, $\alpha = 88.584(9)^\circ$, $\beta = 84.357(9)^\circ$, $\gamma = 89.888(9)^\circ$, $V = 1454.7(13) \text{ \AA}^3$, $Z = 2$, $D_c = 1.615 \text{ g cm}^{-3}$, $F(000) = 720$, $\mu = 2.211 \text{ mm}^{-1}$, 12 526 reflections collected, 6500 unique ($R_{int} = 0.0195$), final $R1 = 0.0547$, $wR2 = 0.1068$, $S = 1.004$ for all data. Crystal data for **2**: $C_{33}H_{30}Cu_6N_{12}$, $M_r = 975.99$, monoclinic, space group $C2/c$ (No. 15), $a = 24.561(4) \text{ \AA}$, $b = 20.118(3) \text{ \AA}$, $c = 8.0845(12) \text{ \AA}$, $\beta = 106.176(2)^\circ$, $V = 3836.6(10) \text{ \AA}^3$, $Z = 4$, $D_c = 1.690 \text{ g cm}^{-3}$, $F(000) = 1944$, $\mu = 3.306 \text{ mm}^{-1}$, 9980 reflections collected, 3377 unique ($R_{int} = 0.0327$), final $R1 = 0.0686$, $wR2 = 0.1393$, $S = 1.171$ for all data. Data collections ($2\theta \leq 56^\circ$) were performed on a Bruker Smart Apex CCD diffractometer (Mo $K\alpha$, $\lambda = 0.71073 \text{ \AA}$) at $T = 298(2) \text{ K}$ using SMART.

(6) (a) Huang, X.-C.; Zheng, S.-L.; Zhang, J.-P.; Chen, X.-M. *Eur. J. Inorg. Chem.* **2004**, 1024–1029. (b) Hu, S.; Zhou, A.-J.; Zhang, Y.-H.; Ding, S.; Tong, M.-L. *Cryst. Growth Des.* **2006**, *6*, 2543–2550.

(7) The first Schläfli symbol of $(6^2 \cdot 10)_2(6 \cdot 10^2)$ topology of **2** is for the $[Cu(Ppz)]_3$ unit and the Cu4 atom and the second for the Cu3 atom. Friedrichs, O. D.; O'Keeffe, M.; Yaghi, O. M. *Acta Crystallogr., Sect. A* **2003**, *59*, 22.

(8) (a) Carlucci, L.; Ciani, G.; Proserpio, D. M.; Rizzato, S. *Chem.—Eur. J.* **2002**, *8*, 1519. (b) Wang, X.-L.; Qin, C.; Wang, E.-B.; Su, Z.-M. *Chem.—Eur. J.* **2006**, *12*, 2680–2691.

0] (24.561 Å), and those belonging to different sets are reachable by each other via a displacement of $[1/2, 1/2, 0]$ (15.874 Å) (Figure S3 in the Supporting Information). Noteworthy is the fact that the inter- Cu_3 $\text{Cu}\cdots\text{Cu}$ distance of **2** (3.317 Å) is even shorter than that of **1**, which suggests a domination of cuprophilicity over the network organization.

For both containing the intrinsic luminophor Cu_3 , **1** and **2** are photoemissive when irradiated by UV rays at room temperature, emitting a bright green light. Especially, upon excitation by 300 nm, **1** exhibits an asymmetric band with $\lambda_{\text{max}} = 564$ nm (Figure S5 in the Supporting Information). The broad band symbolizes a contour of multiple emissions, arising from triplet metal-centered excited states. The assumption is confirmed by the conformity of the band with two Gaussian peaks (505 and 569 nm) ($R^2 = 0.9925$; $\chi^2 = 9.9 \times 10^{-4}$). The band of **1** is similar to that of $[\text{Cu}(\text{3,5-(Me)}_2\text{pz})_3]_3$.^{2a} However, in comparison, its λ_{max} has a hypsochromic shift from the latter (656 nm), and likely for **1**, it has a longer intermolecular $\text{Cu}\cdots\text{Cu}$ contact (3.439 Å) than the reference (2.946 Å).⁹

When excited by 360 nm, **2** also demonstrates an asymmetric band with higher energy ($\lambda_{\text{max}} = 494$ nm) than that of **1**. Accordingly, the band is attributed to metal-centered emissions. A Gaussian fitting gave a fine accord of this band with a mix of high-energy (HE; 492 nm) and low-energy (LE; 548 nm) bands ($R^2 = 0.9891$; $\chi^2 = 1.12 \times 10^{-3}$). With regards to the blue shift of **2** from **1**, a tentative explanation is that the rigidity of the framework of **2** restrains the distortion of excimers,¹⁰ $[\text{Cu}_3]_n$, and thus leads to a smaller Stokes' shift (7530 cm^{-1}) than that for **1** ($15\,600 \text{ cm}^{-1}$).

More surprisingly, upon cooling of the solids of **1** and **2**, both showed a novel chromism, described by the curves in Figure 4 (for more details, see Figures S6 and S7 in the Supporting Information). In particular, as **1** is cooled from room temperature to 150 K, its color changes from yellow-green ($\lambda_{\text{max}} = 564$ nm) to green ($\lambda_{\text{max}} = 505$ nm), and as it is further cooled to 10 K, it turns back to yellow-green ($\lambda_{\text{max}} = 555$ nm). Also, in the same cooling scheme, the color of **2** changes first from green ($\lambda_{\text{max}} = 494$ nm) to bluish-green ($\lambda_{\text{max}} = 486$ nm) and then back to green ($\lambda_{\text{max}} = 498$ nm).

Although the unilateral blue^{2,11} and red¹³ emission shifts of M_3 species with cooling have been well established, the two-directional emission change demonstrated here, to the best of our knowledge, has never been reported. Concerning the red shift of similar Au_3 species,¹³ Burini and his co-workers ascribed it to a cooling-induced cell contraction, a process that enhances the $\text{M}\cdots\text{M}$ interaction. However, concerning the cooling-induced blue shifts of Cu_3 species,² Dias et al. ruled out the possibility that they are caused exclusively by the lattice contraction; instead, he suggested,

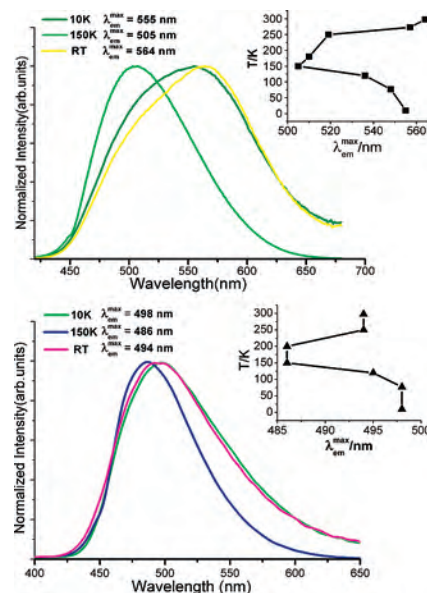


Figure 4. Solid emission spectra of **1** (top) and **2** (bottom) at three different temperatures (10 and 150 K and room temperature). Inset: λ_{max} of **1** and **2** changing with temperature from room temperature to 10 K.

based on the theoretical calculations and the crystal facts of a time-resolved X-ray diffraction analysis,¹² that the chromism is subject to the structural changes of the multiplex excimer. In light of the elegant studies, we can assume the red-after-blue shift to be an effect of two competitive effects that are the contraction of the crystal and the thermal-dominated distortion of excited states. In the range of high temperature, the latter is possibly dominant and so the cooling led to a blue shift of emission, and in the low-temperature range, the former is more prominent, leading to a red shift.

However, it is seen in Figure 1 that the migration of the emission band of **1** with temperature is more dramatic than that of **2**. This is possibly because of the reason, mentioned above, that the more rigid framework of **2** restrains concurrently the volume reduction of the crystal and the distortion of the excimers.

Of course, a persuasive elucidation of the novel thermochromism needs more evidence. Currently, in-depth work is in progress. Anyways, isolation of two new complexes illustrates vividly a strategy using a designed tectonic motif as the functional carrier to fabricate the MOFs with the desired bulk performance. Moreover, the novel luminescence chromisms of **1** and **2** reveal first a profound effect of the temperature on the cuprophilic interactions and photoluminescence of the complexes.

Acknowledgment. This work was financially supported by the Natural Science Foundation of Guangdong Province of China (Grant 04010987).

Supporting Information Available: Crystallographic data in CIF format, additional structural plots, X-ray powder diffraction, and solid luminescence spectra at low temperature. This material is available free of charge via the Internet at <http://pubs.acs.org>.

IC702189F

(13) Burini, A.; Bravi, R.; Fackler, J. P., Jr.; Galassi, R.; Grant, T. A.; Omary, M. A.; Pietroni, B. R.; Staples, R. J. *Inorg. Chem.* **2000**, *39*, 3158–3165.

- (9) (a) Yam, V. W.-W.; Lo, K. K.-W. *Chem. Soc. Rev.* **1999**, *28*, 323. (b) Forward, J. M.; Bohmann, D.; Fackler, J. P., Jr.; Staples, R. *J. Inorg. Chem.* **1995**, *34*, 6330.
 (10) Grimes, T.; Omary, M. A.; Dias, H. V. R.; Cundari, T. R. *J. Phys. Chem. A* **2006**, *110*, 5823–5830.
 (11) (a) Ouellette, W.; Prosvirin, A. V.; Chieffo, V.; Dunbar, K. R.; Hudson, B.; Zubietta, J. *Inorg. Chem.* **2006**, *45*, 9346–9366. (b) Dias, H. V. R.; Diyabalanage, H. V. K.; Rawashdeh-Omary, M. A.; Franzman, M. A.; Omary, M. A. *J. Am. Chem. Soc.* **2003**, *125*, 12072–12073.
 (12) Vorontsov, I. I.; Kovalevsky, A. Y.; Chen, Y. S.; Graber, T.; Gembicky, M.; Novozhilova, I. V.; Omary, M. A.; Coppens, P. *Phys. Rev. Lett.* **2005**, *94*, 193003.